Theor Chem Account (2008) 120:499–506
DOI 10.1007/s00214-008-0445-4

REGULAR ARTICLE

Theoretical modeling of open-shell molecules in solution: a QM/MM molecular dynamics approach

Giuseppe Brancato · Nadia Rega · Mauro Causà · Vincenzo Barone

Received: 21 November 2007 / Accepted: 31 March 2008 / Published online: 29 April 2008

Abstract In this work, the GLOB model, an effective and reliable computational approach well suited for ab initio and QM/MM molecular dynamics simulations of complex molecular systems in solution, has been applied to study two representative open-shell systems, the cobalt(II) ion and the glycine radical in aqueous solution, with special reference to their structural and magnetic properties. The main structural features of the solvent cage around the cobalt ion and the hydrogen bonding patterns around the neutral and zwitterionic forms of the glycine radical have been investigated in some detail. The general good agreement with experiments supports the use of the present model to investigate more challenging and biological/technological relevant open-shell systems.

Keywords Open-shell · Molecular dynamics · Continuum models · Cobalt · Glycine radical

1 Introduction

The accurate theoretical modeling of open-shell systems in solution, such as radicals or high-spin transition metal complexes, still represents a challenge due to the delicate balance among intramolecular and intermolecular interactions, as well as electronic rearrangements [1–3]. Moreover, the treatment of both dynamical and environmental effects usually requires the use of molecular dynamics (MD) techniques. In order to illustrate recent progresses in this field we have selected two representative cases connected with different spectroscopic techniques, namely aqueous solutions of the cobalt ion (related to EXAFS spectroscopy), and of the carbon-centered aliphatic radical issuing from elimination reactions involving the simplest amino acid, glycine (related to EPR spectroscopy). Although a number of features have been analyzed for both systems, interpretation of experimental results is not without ambiguities both because of the role of different environmental effects and because the relationship between spectroscopic and structural/dynamics characteristics is only indirect. Explicit/implicit models [4–6] rooted into density functional theory are attractive for the computation of averaging effects brought about by dynamics when a spectroscopic transition is fast with respect to the time scale of a dynamical phenomenon. In such circumstances MD simulations are able to take into account at the same time solvent librations and solute vibrations, both of which can lead to non-negligible averaging effects of spectroscopic parameters. In the absence of significant solute–solvent electron or spin transfer, an integrated approach in which a full quantum mechanical (QM) description of the solute is coupled to a molecular mechanics (MM) modeling of a few water shells embedded in proper boundaries represents the most effective and reliable solution due to the existence of very reliable force fields for water that can reproduce satisfactory bulk behavior, providing results in good agreement with more demanding full QM simulations [7, 8]. Thus all short-time dynamical effects in solution should be well accounted for by reliable QM/MM/implicit solvent approaches [9–13]. Here, we have used the general liquid optimized boundary (GLOB) model [14–16], an effective discrete/continuum theoretical model particularly well suited for treating molecular liquids and/or solute–solvent systems of variable size and at different levels of theory, such

Contribution to the Nino Russo Special Issue.

G. Brancato (✉) · N. Rega (✉) · M. Causà · V. Barone
Dipartimento di Chimica and INSTM, Università Federico II, Complesso Monte S. Angelo, Via Cintia, 80126 Naples, Italy
e-mail: gbrancato@unina.it

N. Rega
e-mail: nadia.rega@unina.it

as MM, QM/MM, and full QM methodologies. According to this model, an explicit molecular system is embedded into the cavity of a dielectric continuum, which represents implicitly the surrounding bulk liquid, and simulated in a canonical ensemble using molecular dynamics techniques. Remarkably, the GLOB model accounts for the interactions with bulk solvent (continuum) considering both short-range dispersion–repulsion and long-range electrostatic contributions, allowing a consistent thermodynamic behavior of the explicit system even in proximity of the cavity boundaries.

Similar discrete/continuum approaches have been proposed also by other authors [10,12,13], starting from the pioneering work of Warshel [9], where the differences about all such methods concern mainly the electrostatic (long-range) and the boundary (short-range) treatments. In particular, the latter should be designed to moderate the possible appearance of spurious boundary effects at the interface between the explicit system and the continuum, which could perturb the explicit solvent dynamics with respect to bulk behaviour. To this end, a number of different approaches have been proposed in previous studies [10,17–20]. The GLOB model adopts an effective representation of the short-range (dispersion and repulsion) interactions derived so as to minimize edge effects on the solvent density, angular orientation and average energy [16,21,22]. On the other hand, the electrostatic interactions with the environment are effectively evaluated according to the conductor-like polarizable continuum model (C-PCM) [23,24], which is one of the most robust and sophisticated models devised to include the reaction potential in the electronic Hamiltonian [25,26] allowing the definition of molecular energy in solution through a variational problem and the implementation of very effective algorithms for the evaluation of analytical energy derivatives in solution.

As mentioned above, in the present work we will analyze aqueous solutions of the divalent cobalt ion and the zwitterionic form of the glycine radical (NH_3^+–CH–COO^-). The Co(II) ion was considered in a quartet state, corresponding to the experimental spin state [27] and in agreement with previous calculations [28]. In both cases, the solute was treated at DFT B3LYP level [29,30], whereas the solvent was modeled as TIP3P [31] water. However, for the Co(II) ion simulation also the first solvation shell, i.e., six water molecules, was treated at full QM level, in order to accurately model the delicate charged ion-solvent interactions without any a priori assumption. Therefore, we focus here on the structural features of the Co(II)–$(H_2O)_6$ complex on the basis of previous experimental [32,33] and theoretical works [28] that have shown how such a complex is very stable in solution and water exchange does occur on a relatively long time scale (10^{-6}–10^{-7} s) with respect to the time interval considered in the present work (10^{-12} s). Reported results show that both environmental and dynamical effects can be reliably studied using the present integrated approach and, in addition, important spectroscopic parameters could be obtained in remarkable agreement with the corresponding experimental counterparts.

This paper is organized as follows: In Sect. 2, a brief overview of the GLOB model is presented and all required computational details are provided. In Sect. 3, we report a detailed structural analysis of the cobalt ion and glycine radical in aqueous solutions issuing from the corresponding QM/MM GLOB simulations at room temperature. Therein, a comparison with available spectroscopic experimental data is also provided. Finally, concluding remarks are given in Sect. 4.

2 Methods

2.1 GLOB model

The GLOB model is based on the combination of quantum mechanical methods, molecular dynamics techniques and continuum models. The general features of the GLOB model have been described in full detail in Refs. [14–16]. Here, we will briefly sketch the basic idea and the most significant aspects of the model. According to the present model, an explicit molecular system is embedded into the cavity of a dielectric continuum, which accounts for the interactions with the environment. Such non-periodic boundary conditions are particularly well suited for treating solute–solvent systems, which are intrinsically non-periodic, avoiding possible correlation effects that may occur with standard PBC methodologies [5,34–39]. The molecular system can be treated by standard force field based models, high-level quantum mechanical methods or mixed quantum mechanics/molecular mechanics models. In the most general case, the system is described by an effective Hamiltonian composed by an "high level" region, treated at full quantum mechanical level (e.g., representing the solute and, possibly, a few solvent molecules) and a "low level" region treated by a molecular mechanics force field, providing an electrostatic embedding (generated by their charge distribution) of the quantum core region (see Fig. 1). Moreover, interactions with bulk solvent (continuum) take into account both an exact treatment of the electrostatic reaction field [24] and an effective representation of short-range (dispersion and repulsion) interactions via an optimized mean force potential [16,21,22]. The latter also includes terms of electrostatic origin (reaction field) not fully accounted for by intrisically approximated continuum models [16], due to the lack of specific solvent (explicit)–solvent (implicit) hydrogen-bond interactions that could induce anisotropic distributions of the molecular orientation in proximity of the cavity surface [10,21]. As a result, such a potential does remove effectively unwanted physical anisotropies of the solvent, such as the non-

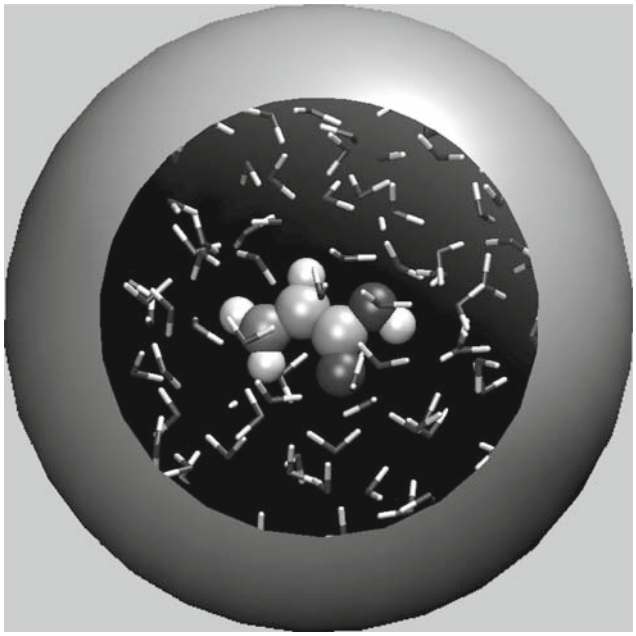

Fig. 1 Graphical representation of a molecular system (glycine radical + water) simulated using the GLOB model

uniform distribution of the density and the artificial solvent polarization due to the partial alignment of the molecular dipoles at the boundary [16].

Hence, introducing formally the one-electron density matrix, **P**, to describe the explicit system, we can express the free energy $A(\mathbf{x})$ at a specific nuclear configuration, **x**, as:

$$A(\mathbf{x}) = E(\mathbf{P}, x) + W_{\text{elec}}(\mathbf{P}, x) + W_{\text{dis-rep}}(x) \quad (1)$$

where $E(\mathbf{P}, x)$ is the potential energy of the explicit system in the nuclear configuration x, W_{elec} and $W_{\text{dis-rep}}$ are, respectively, the long and short-range parts of the mean field, as mentioned above; the one-electron density matrix, **P**, mutually polarized by the bulk (continuum), can be obtained via the self-consistent field (SCF) solution of an electronic Hamiltonian which includes the mean field operator as an effective term [25,26], whereas $W_{\text{dis-rep}}$ is an average potential obtained empirically and not depending on **P**. In particular, in the GLOB model, W_{elec} is provided by the effective CPCM [40,24], corresponding to the PCM [41] limit for infinite dielectric constant, but used with satisfactory results also for solvent of rather low polarity. As a result, a consistent mean force potential governing the dynamics of the explicit system can be used to carry out NVT molecular dynamics simulations within the Born–Oppenheimer [42,43] or the extended-Lagrangian [44–47] frameworks. In the present work, we consider the atom centered density matrix propagation (ADMP) [45–47] method, in which the density matrix of the atomic basis set evolves "on-the-fly" together with the nuclei as a dynamic variable. Accordingly, the polarization of the dielectric continuum is updated at each MD step based on the total charge distribution of the explicit system (QM electron density and MM point charges).

2.2 Computational details

All the room temperature QM/MM molecular dynamics simulations reported in the present work were performed according to the GLOB/ADMP model, as described in the preceding section. Core and valence orbitals were weighted differently, through the corresponding electron density matrix, with a fictitious mass of $\mu_{\text{valence}} = 0.1\,\text{amu bohr}^2 \approx 180$ a.u. for the valence electrons and μ_{core} obtained according to the tensorial fictitious mass scheme described in Ref. [46]. A constant thermal energy has been enforced by scaling nuclear velocities every 2,500 steps, with a time step of 0.2 fs.

In the simulation of the Co(II) ion in aqueous solution, the metal ion along with its first solvent shell (six water molecules) was treated at B3LYP [29,30] level (QM region) and solvated with 139 TIP3P water molecules (MM region). Also, based on previous calculations [28] the ground state of the cobalt ion in solution has been considered to be the quartet state. A standard Lennard–Jones potential has been used to model the non-electrostatic interactions, where the Co(II)–H_2O^{MM} parameters were taken from Ref. [48] and the H_2O^{QM}–H_2O^{MM} parameters were optimized to reproduce the TIP3P water dimer structure and energetics [49]. Similarly, in the glycine radical simulation, the solute was treated full quantum mechanically (B3LYP) and the solvent modeled as TIP3P water (134 molecules). Interactions between QM and MM parts, as usual, consist of both electrostatic and van der Waals interactions, where the latter are approximated according to the B3LYP/TIP3P potential parametrized by Freindorf et al. [50] In both cases, the explicit molecular system was embedded into a spherical cavity of a dielectric medium with a radius of 11.8 Å. The center of mass of the solute was constrained at the center of the cavity.

We have paid special attention to the development of a general purpose basis set, hereafter referred as N07D (acronym of "Naples 2007"), particularly well suited for ab initio molecular dynamics, which provides comparable results in terms of molecular geometries and electric dipole moments to more extended basis sets. In particular, such basis set has been obtained from a re-optimization of the 6-31G* basis set with the addition of an s function to the core-valence region and p, d diffuse functions to the heavy atoms. Details of the N07D basis set, along with various comparative tests, can be found in Ref. [51] In the present work, the glycine radical and the water molecules around the cobalt ion were treated with the N07D basis set, while for the Co(II) ion we have decided to employ the LANL2DZ effective core potentials and valence basis sets, in agreement with previous

studies [28,52]. All the quantum mechanical calculations and the QM/MM molecular dynamics simulations have been performed with a modified version of the Gaussian package [53].

3 Results and discussion

3.1 Cobalt ion

We present preliminary results of a 5 ps QM/MM molecular dynamics simulation of the cobalt ion in aqueous solution at room temperature. In Fig. 2, we report the Co–O and Co–H radial distribution functions (RDFs). The first two narrow peaks of the RDFs are located at about 2.11 and 2.73 Å, for oxygen and hydrogen, respectively. It is worth noting that from quantum mechanical calculations of the optimized structure of the Co(II)–$(H_2O)_6$ cluster with or without the inclusion of solvent effects via the C-PCM, we have obtained a Co–O distance of 2.10 and 2.12 Å, respectively. Therefore, molecular dynamics and cluster calculations do provide consistent results and, as observed in previous studies of metal ions, solvent effects induce a shortening of the metal ion–water distance. Remarkably, the present Co–O distance is also in close agreement with recent EXAFS experiments (2.09 Å) [32]. The running integration function (see Fig. 2a) shows that the number of water molecules in the first solvation shell is six up to a distance of about 3.5 Å. In the first solvent shell, no water exchange does occur during the simulation, while a more dynamical picture is observed in the second shell, as indicated by the broader second Co–O and Co–H RDF's peaks. Also, we have analyzed the coordination number distributions around the cobalt ion (see Fig. 3). In order to define the coordination number for each molecular configuration, we have considered the distance ranges of 0.0–3.0 Å and 3.1–4.8 Å for the first and second solvent shell, respectively. As shown in Fig. 3, for the first shell the distribution provides only a coordination number of 6 water molecules, whereas for the second shell we observe a population ranging between 12 and 16 water molecules.

Furthermore, we have evaluated the root mean square deviations (RMSD) of the Co(II)–$(H_2O)_6$ complex (including only the heavy atoms: Co, O) in aqueous solution from an ideal octahedral conformation, as issuing from the GLOB molecular dynamics simulation. The RMSD computed along the last 4 ps reported in Fig. 4, shows that a quasi-symmetric structure of the 6-coordinated cluster is retained during the whole simulation time interval, i.e., deviations are, overall, less than 0.3 Å. Finally, we have considered the angular distribution of the water molecules in the first and second solvent shell relative to the metal ion. The angle (θ) formed between the water dipole moments and the vector pointing along the Co–O direction has been used in the present analysis. As

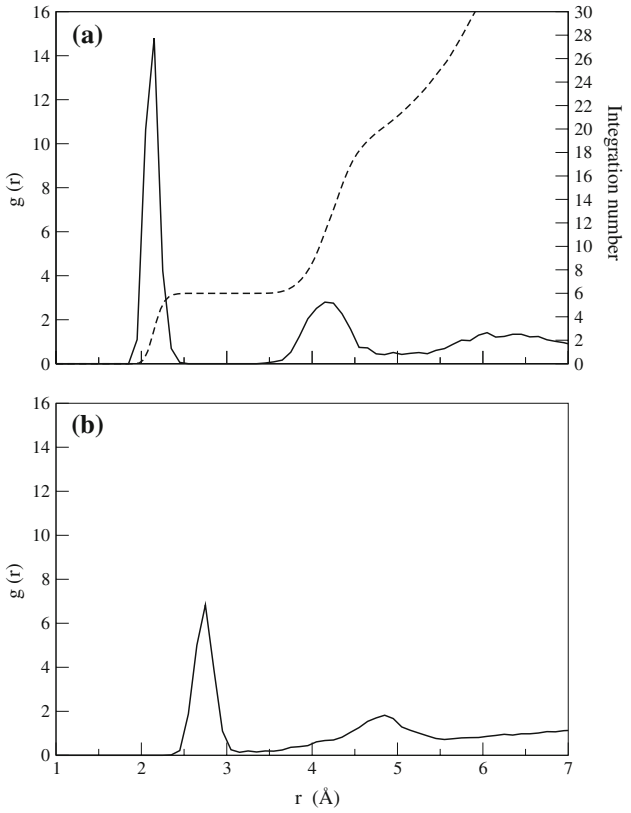

Fig. 2 **a** Co–O RDF (*solid line*), along with its running integration number (*dashed line*), and **b** Co–H RDF issuing from the GLOB MD simulation

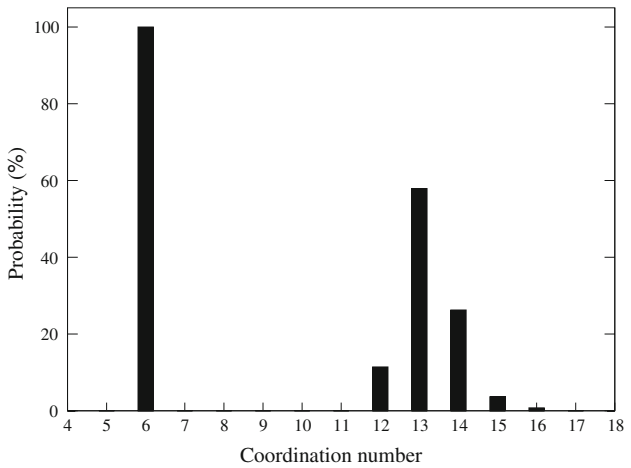

Fig. 3 Coordination number distributions of the first and second solvent shells of the Co(II) ion in aqueous solution issuing from the GLOB MD simulation

observed also in other studies [54,55], the water molecules in direct contact with the metal ion are slightly tilted with respect to the linear angle ($\theta = 180°$), showing an angular distribution centered at about 155°, as shown in Fig. 5. Such a local solvent structure is still present in the second shell, even if the angular distribution gets broader, indicating

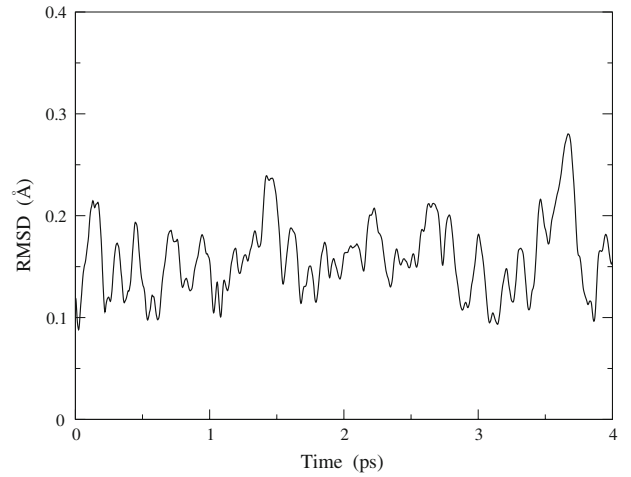

Fig. 4 Root mean square deviations (RMSD) of the Co(II)–$(H_2O)_6$ cluster (including only the heavy atoms: Co, O) from the ideal symmetric (octahedral) conformation issuing from the GLOB MD simulation

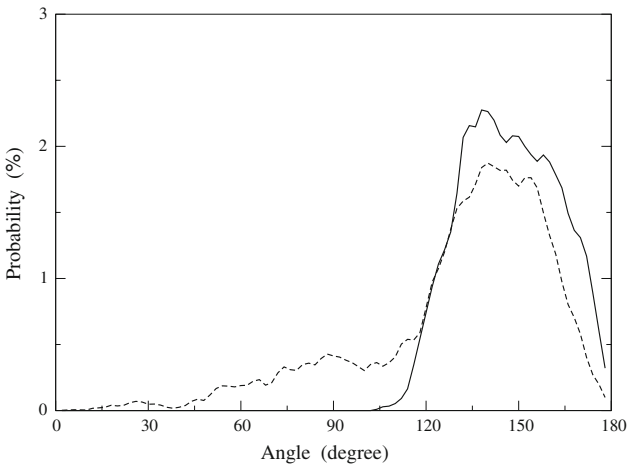

Fig. 5 Angular distributions of the first (*solid line*) and second (*dashed line*) solvent shell of the Co(II) ion in aqueous solution issuing from the GLOB MD simulation

that, in terms of molecular orientation, the bulk behavior is reached at a longer distance, presumably beyond the third shell.

3.2 Glycine radical

As an example of biologically relevant open shell systems, we have selected the radical issuing from the homolytic breaking of the C^{α}–H^{α} bond of the simplest amino acid, glycine, that has shown a number of unexpected features (e.g., preference for zwitterionic or non-zwitterionic form in different environments, anomalously low hydrogen hyperfine coupling in aqueous solution). This has stimulated a large number of experimental [56–60] and theoretical [3,61–63] studies. In a previous work [8], we have shown how a combined theoretical approach, based on the GLOB model and post-MD quantum mechanical calculations, is able to provide important insights of the dynamical and environmental effects of the glycine radical in aqueous solution in connection with its magnetic properties. In particular, it has been shown that static cluster models could not provide a reliable picture of the solute-solvent conformation in solution. Here, we want to focus on the most important structural aspects of the zwitterionic form (NH_3^+–CH–COO^-, hereafter $GlyR^{zw}$) of the glycine radical, which were not discussed in Ref. [8] being $GlyR^{zw}$ a less stable isomer in aqueous solution at not too basic pH with respect to the neutral form (NH_2–CH–COOH, hereafter GlyR). This is in contrast to the parent molecule that shows a clear preference for the zwitterionic form in solution [64–66].

In the following, the differences between $GlyR^{zw}$ and GlyR, as obtained from QM/MM GLOB simulations of the two species in aqueous solution, will be considered, as well as a comparison of computed and experimental EPR hyperfine coupling constants (hfc).

It is well known that the zwitterionic form of the glycine radical is unstable in the gas-phase (molecular optimization leads to the neutral form) but it can exist in a more favorable polar environment, e.g., it has been detected experimentally in the solid state [67], and might be present also in aqueous solution, even if at much lower concentration with respect to the preferred neutral form.

In Fig. 6, the gas-phase optimized structures and atom labels of GlyR and $GlyR^{zw}$ are depicted, along with the corresponding singly occupied molecular orbitals (SOMOs), as computed at the B3LYP/EPR-II level. Note that in the optimization of $GlyR^{zw}$, the N–C^{α}–C angle has been constrained to 117.6°. In both cases, the delocalization effects of the unpaired electron induce an almost planar structure of the radical, with the exception of the aminic hydrogens. GlyR shows a slightly pyramidal aminic group, with $\phi(\mathrm{H1NC^{\alpha}C}) = -9.5°$ and $\phi(\mathrm{H2NC^{\alpha}C}) = -165.0°$, whereas H^{α} is on the same plane of the N–C^{α}–C group [$\phi(\mathrm{NH^{\alpha}CC^{\alpha}}) = 1.6°$]. Moreover, while GlyR shows a delocalized character of the SOMO centered on the C^{α} atom, in $GlyR^{zw}$ the electron delocalization is hindered by a different hybridization of the nitrogen atom. On the other hand, in aqueous solution GlyR is, on average, planar: the fluctuations of the aminic hydrogens are symmetrically distributed about the molecular plane, as shown in Table 1, and no rotation of the NH_2 group has been observed. The N–C^{α} and C^{α}–C bonds are slightly contracted in going from the gas-phase to the condensed phase, whereas the N–H, C^{α}–H, C=O and O–H bonds are elongated. Concerning $GlyR^{zw}$, the main intramolecular changes involve the shortening of the C^{α}–C bond and the symmetrization of the NH_3 and CO_2 groups: the three N–H bonds and the two C=O1 and C=O2 bonds become basically equivalent due to the interactions with water and the breaking of the weak N–H1–O1=C hydrogen bond.

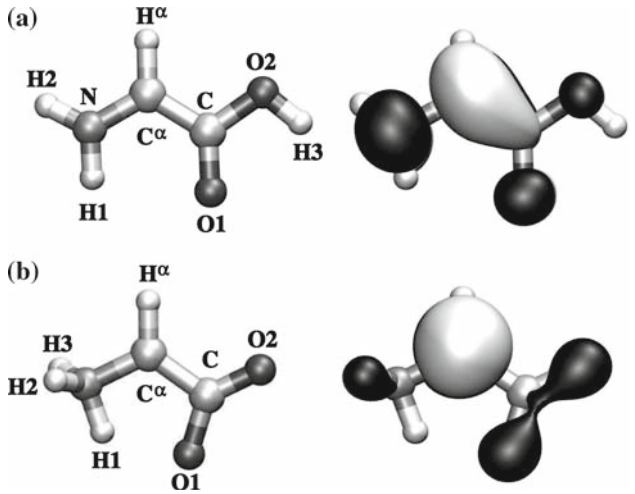

Fig. 6 Optimized gas-phase structures, labels and SOMOs of **a** GlyR and **b** GlyR^{zw}. A threshold of 0.05 has been used to plot the orbitals

Table 1 Geometrical parameters of the glycine radical (GlyR and GlyR^{zw}) issuing from gas-phase (GP) optimizations and aqueous solution (Sol) simulations

GlyR	GP	Sol	GlyR^{zw}	GP	Sol
N–H1	1.013	1.017	N–H1	1.040	1.041
N–H2	1.008	1.016	N–H2	1.040	1.041
N–C$^{\alpha}$	1.358	1.353	N–H3	1.040	1.041
C$^{\alpha}$–H$^{\alpha}$	1.082	1.086	N–C$^{\alpha}$	1.455	1.457
C$^{\alpha}$–C	1.429	1.426	C$^{\alpha}$–H$^{\alpha}$	1.087	1.086
C=O1	1.228	1.242	C$^{\alpha}$–C	1.485	1.479
C–O2	1.367	1.366	C=O1	1.281	1.266
O2–H3	0.970	0.984	C=O2	1.231	1.262
H1–N–H2	117.7	116.7	H1–N–H2	110.8	107.0
N–C$^{\alpha}$–C	118.2	120.3	H2–N–H3	108.6	107.0
NH$^{\alpha}$CC$^{\alpha}$	1.6	0.0	H1–N–H3	110.8	107.0
H1NC$^{\alpha}$C	–9.5	1.3	N–C$^{\alpha}$–C	117.6	117.7
H2NC$^{\alpha}$C	–165.0	–179.8	NH$^{\alpha}$CC$^{\alpha}$	0.0	0.4
μ	2.79	4.20	μ	10.5	14.1

Bond distances are in Å, angles in degrees

Furthermore, the solute–solvent structural arrangement has been analyzed in detail. In Fig. 7, the spatial distribution function (SDF) of the solvent molecules surrounding the glycine radical is depicted. Both isomers do form hydrogen bonds with their terminal groups, the C$^{\alpha}$–H$^{\alpha}$ moiety being rather hydrophobic. Also, we note that the ammonium group of GlyR^{zw} can freely rotate and, therefore, the water molecules are spherically distributed with respect to the N–C$^{\alpha}$ axis. On the other hand, within the simulation time interval we have not observed any significant rotation of the carboxyl group in both glycine radical forms. From an hydrogen bond analysis, we have obtained that each hydrogen atom of the NH_3^+ or NH_2 group does form, on average, about one

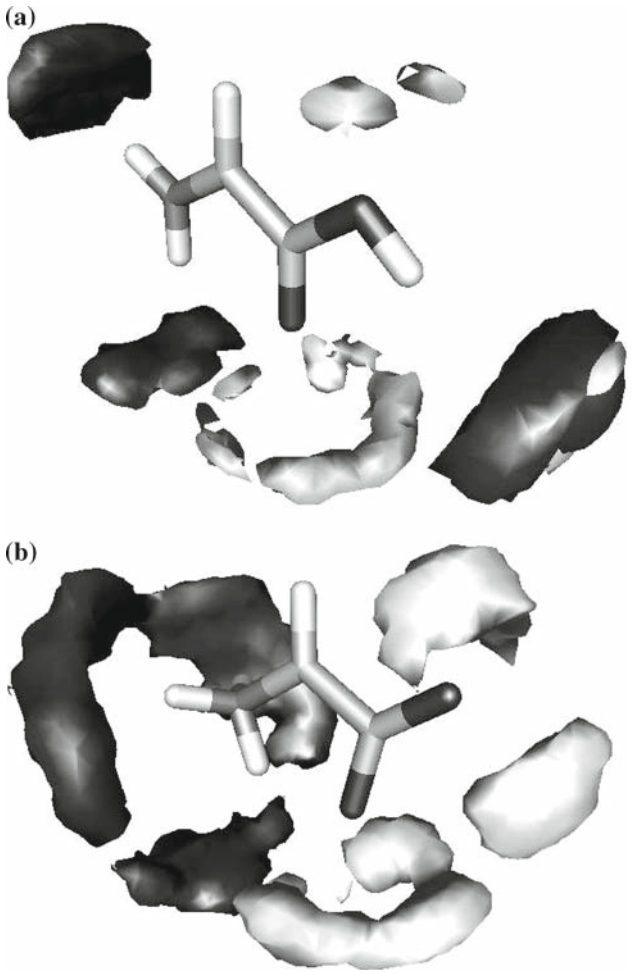

Fig. 7 Spatial distribution functions of water molecules around the **a** NH_2–CH–COOH and **b** NH_3^+–CH–COO^- radicals issuing from GLOB simulations. *Light grey*, water hydrogen atoms; *dark grey*, water oxygen atoms

Table 2 Average number of hydrogen bonds between glycine radical (GlyR and GlyR^{zw}) and water issuing from GLOB simulations

GlyR		GlyR^{zw}	
H-bond donor			
H1	0.6	H1	1.1
H2	0.7	H2	1.2
H3	1.0	H3	1.0
H-bond acceptor			
O1	2.1	O1	2.7
O2	0.8	O2	3.0

hydrogen bond with a water molecule (see Table 2). Moreover, hydrogen bonds of COO^- with water are more directional and each oxygen forms up to three hydrogen bonds.

Let us now consider the hfc's issuing from a posteriori quantum mechanical calculations on selected molecular configurations of the GlyR^{zw} simulation. To this end, the

Table 3 Isotropic hyperfine coupling constants (Gauss) issuing from GLOB simulation, DFT-PBC crystal calculations and experiments

Atom	Solution	Crystal	Exp
C^{α}	38.0	39.1	45.2[a]
H^{α}	−22.8	−24.0	−22.7[b]
N	−3.0	−3.0	−3.1[c]
H(N)	18.7	17.9	17.5[b]

[a] Ref. [57]
[b] Ref. [60]
[c] Ref. [56]

purposely tailored EPR-II basis set has been employed in combination with the B3YLP method and the hfcs have been obtained from statistical averages of the corresponding parameters. Results are reported in Table 3 and compared with the only available experimental data, which are recorded in the solid state, and with recent calculations of the $GlyR^{zw}$ radical embedded in α-glycine crystal [68]. The latter specifically consist of DFT-PBC calculations performed on a unit cell, previously optimized, containing the $GlyR^{zw}$ radical and other 11 glycine molecules. Overall, we observe a remarkable agreement between computed and experimental data, the only exception being the C^{α} radical center that is known to be underestimated by DFT computations. Note that, due to the free rotation of the NH_3^+ group at room temperature in both liquid and solid phases, only one average value has been provided for the hfc of the three hydrogen atoms directly linked to N.

4 Conclusions

In this work, a recently developed computational model, referred to as GLOB, well suited for first-principle simulations of molecular liquids has been applied to study two prototype open-shell systems, the cobalt ion and the glycine radical in aqueous solution, which already present some of the most important features of more complex molecular systems. In both cases, the need of an accurate quantum mechanical treatment of the solute is apparent, being standard molecular mechanics methods not appropriate to model such systems. Here, the GLOB model has allowed to use an effective and reliable hybrid QM/MM scheme, where the relevant part of the system, i.e., the solute with at most a few solvent molecules, has been treated with the well-trusted B3LYP method, while the rest of the system has been conveniently modeled with the TIP3P water model. Interactions between the explicit system and the environment (implicit solvent) are taken into account via a continuum model, which properly includes both short-range dispersion–repulsion and long-range electrostatics contributions. Remarkably, first-principle molecular dynamics can be performed efficiently by following an extended-Lagrangian scheme using localized basis functions, allowing the GLOB model to be considered a promising alternative, especially for non-periodic systems, such as liquids and solutions, to other standard molecular dynamics methods, like the Car-Parrinello approach.

In the illustrative applications, the main structural features governing the solute–solvent conformational arrangements have been investigated in full detail. In particular, the characteristic cobalt ion-water interaction distance has been found in close agreement with recent EXAFS experiments. In this case, due to the high stability of the Co(II)–$(H_2O)_6$ complex and the need for an accurate treatment of the solute–solvent interactions, the first solvent shell was treated at full ab initio level. Moreover, the environmental and dynamical effects modulating the structure of the zwitterionic form of the glycine radical in solution have been analyzed from the GLOB simulation. In addition, a posteriori quantum mechanical calculations of relevant EPR parameters, i.e. hyperfine coupling constants, have been also carried out. Remarkably, computational results have nicely matched the available experimental counterparts.

It is worth noting that one of the main goal of sophisticated MD techniques concerns the evaluation of accurate solvation free energies of complex solutes [69,70]. However, the sensitivity of the free energy with the potential energy surface and the slow convergence with the number of sampled molecular configurations make this calculation a challenging task, as far as expensive quantum mechanical methods are employed, without the use of "ad hoc" computational approaches. Currently, we are working to develop an efficient strategy based on the GLOB model in order to address such an important and difficult issue.

In conclusion, we think that the flexibility and effectiveness of the GLOB model allow to study more challenging chemical systems in solution, such as magnetically active biological macromolecules, providing that the time scale of the processes involved are compatible with the time interval now accessible with standard computational facilities.

Acknowledgments The financial support of MIUR and INSTM is gratefully acknowledged. All the calculations have been performed at "Campus Computational Grid"-Università di Napoli "Federico II" advanced computing facilities.

References

1. Barone V, Adamo C (1994) Chem Phys Lett 224:432
2. Barone V (1995) J Phys Chem 99:11659
3. Rega N, Cossi M, Barone V (1997) J Am Chem Soc 119:12962
4. Okur A, Simmerling C (2006) Annual reports in computational chemistry. Hybrid explicit/implicit solvation methods. vol 2 Elsevier, Amsterdam
5. Warshel A, Sharma PK, Kato M, Parson WW (2006) Biochim Biophys Acta 1764:1647

6. Roux B, Simonson T (1999) Biophys Chem 78:1
7. Brancato G, Rega N, Barone V (2006) J Chem Phys 125:164515
8. Brancato G, Rega N, Barone V (2007) J Am Chem Soc 129:15380
9. Warshel A (1978) Chem Phys Lett 55:454
10. King G, Warshel A (1989) J Chem Phys 91:3647
11. Rega N, Iyengar SS, Voth GA, Schlegel HB, Vreven T, Frisch MJ (2004) J Phys Chem B 108:4210
12. Im W, Bernche S, Roux B (2001) J Chem Phys 114:2924
13. Schaefer P, Ricciardi D, Cui Q (2005) J Chem Phys 123:014905
14. Rega N, Brancato G, Barone V (2006) Chem Phys Lett 422:367
15. Brancato G, Barone V, Rega N (2007) Theor Chem Acc 117:1001
16. Brancato G, Rega N, Barone V (2008) J Chem Phys 128:144501
17. Brooks CL, Karplus M (1983) J Chem Phys 79:6312
18. Beglov D, Roux B (1994) J Chem Phys 100:9050
19. Essex JW, Jorgensen WL (1995) J Comput Chem 16:951
20. Attard P (2006) Mol Phys 104:1951
21. Brancato G, Di Nola A, Barone V, Amadei A (2005) J Chem Phys 122:154109
22. Brancato G, Rega N, Barone V (2006) J Chem Phys 124:214505
23. Klamt A, Schüurmann G (1993) J Chem Soc Perkin Trans 2:799
24. Cossi M, Rega N, Scalmani G, Barone V (2003) J Comp Chem 24:669
25. Tomasi J, Persico M (1994) Chem Rev 94:2027
26. Tomasi J, Mennucci B, Cammi R (2005) Chem Rev 105:2999
27. Cotton FA, Wilkinson G (1980) Advanced inorganic chemistry. Wiley, New York
28. Chillemi G, D′Angelo P, Pavel NV, Sanna N, Barone V (2002) J Am Chem Soc 124:1968
29. Becke AD (1993) J Chem Phys 98:5648
30. Stephens PJ, Devlin FJ, Chabalowski CF, Frisch MJ (1994) J Phys Chem 98:11623
31. Jorgensen WL, Chandrasekhar J, Madura JD, Impey RW, Klein ML (1983) J Chem Phys 79:926
32. D′Angelo P, Barone V, Chillemi G, Sanna N, Meyer-Klaucke W, Pavel NV (2002) J Am Chem Soc 124:1958
33. Miyanaga T, Sakane H, Watanabe I (1995) Bull Chem Soc Jpn 68:819
34. Smith PE, Pettitt BM (1991) J Chem Phys 95:8430
35. Smith PE, Pettitt BM (1996) J Chem Phys 105:4289
36. Smith PE, Blatt HD, Pettitt BM (1997) J Phys Chem B 101:3886
37. Hunenberger PH, McCammon JA (1999) J Chem Phys 110:1856
38. Bergdorf M, Peter C, Hunenberger PH (2003) J Chem Phys 119:9129
39. Bogusz S, III TEC, Brooks BR (1998) J Chem Phys 108:7070
40. Barone V, Cossi M (1998) J Phys Chem A 102:1995
41. Miertuš S, Scrocco E, Tomasi J (1981) Chem Phys 55:117
42. Bolton K, Hase WL, Peslherbe GH (1998) Modern methods for multidimensional dynamics computation in chemistry. Direct Dynamics of Reactive Systems, World Scientific, Singapore, p 143
43. Millam JM, Bakken V, Chen W, Hase WL, Schlegel HB (1999) J Chem Phys 111:3800
44. Marx D, Hutter J (2000) Modern methods and algorithms of quantum chemistry, Ab initio molecular dynamics: theory and implementation. vol. 1 (John vonNeumann Institute for Computing, Julich), p 301
45. Schlegel HB, Millam JM, Iyengar SS, Voth GA, Daniels AD, Scuseria GE, Frisch MJ (2001) J Chem Phys 114:9758
46. Iyengar SS, Schlegel HB, Millam JM, Voth GA, Scuseria GE, Frisch MJ (2001) J Chem Phys 115:10291
47. Schlegel HB, Iyengar SS, Li X, Millam JM, Voth GA, Scuseria GE, Frisch MJ (2002) J Chem Phys 117:8694
48. Babu CS, Lim C (2006) J Phys Chem A 110:691
49. Brancato G, Rega N, Barone V (2008) Chem Phys Lett 451:53
50. Freindorf M, Shao Y, Furlani TR, Kong J (2005) J Comput Chem 26:1270
51. Barone V, Cimino P, Stendardo E (2008) J Chem Theory Comp (in press)
52. Rotzinger FP (2005) J Phys Chem B 109:1510
53. Frisch MJ, Trucks GW, Schlegel HB, et al. (2003) Gaussian 03, revision c.02. Gaussian, Inc.
54. Mohammed AM, Loeffler HH, Inada Y, Tanada K, Funahashi S (2005) J Mol Liq 119:55
55. Fatmi MQ, Hofer TS, Randolf BR, Rode BM (2005) J Chem Phys 123:054514
56. Ghosh DK, Wiffen DH (1960) J Chem Soc: 1869:1869
57. Morton JR (1964) J Am Chem Soc 86:2325
58. von Paul H, Fisher H (1971) Helv Chim Acta 54:485
59. Neta P, Fessenden RW (1971) J Phys Chem 75:738
60. Sanderud A, Sagstuen E (1998) J Phys Chem B 102:9353
61. Barone V, Adamo C, Grand A, Brunel Y, Fontecave M, Subra R (1995) J Am Chem Soc 117:1083
62. Wood GPF, Moran D, Jacob R, Radom L (2005) J Phys Chem A 119:6318
63. Kaprzac S, Reviakine R, Kaupp M (2007) J Phys Chem B 111:811
64. Warshel A (1979) J Phys Chem 83:1640
65. Bandyopadhyay P, Gordon MS, Mennucci B, Tomasi J (2002) J Chem Phys 116:5023
66. Aikens CM, Gordon MS (2006) J Am Chem Soc 128:12835
67. Ghosh DK, Whiffen DH (1959) Mol Phys 2:285
68. Barone V, Causà M (2008) Chem Phys Lett 452:89
69. Luzhkov V, Warshel A (1992) J Comput Chem 13:199
70. Olson MHM, Hong G, Warshel A (2003) J Am Chem Soc 125:5025